Composite Structures 289 (2022) 115440

Contents lists available at ScienceDirect

Composite Structures

journal homepage: www.elsevier.com/locate/compstruct

A combined experimental and micromechanical approach to investigating PTC and NTC effects in CNT-polypropylene composites under a self-heating condition

Taegeon Kil [a], D.W. Jin [a], Beomjoo Yang [b], H.K. Lee [a,*]

[a] Department of Civil and Environmental Engineering, Korea Advanced Institute of Science and Technology (KAIST), 291 Daehak-ro, Yuseong-gu, Daejeon 34141, Republic of Korea
[b] School of Civil Engineering, Chungbuk National University, 1 Chungdae-ro, Seowon-gu, Cheongju, Chungbuk 28644, Republic of Korea

ARTICLE INFO

Keywords:
Conductive polymeric composites
Carbon nanotube
Self-heating
Micromechanics
Molecular dynamics

ABSTRACT

The present study proposed a combined experimental and micromechanical approach to investigating positive temperature coefficient (PTC) and negative temperature coefficient (NTC) effects in carbon nanotube (CNT)-polypropylene composites under a self-heating condition. The electrical and heating performance of the composites were investigated by electrical conductivity measurements and self-heating tests with various input voltages. The test results showed that composites with a CNT content of 5.0 wt.% exhibited excessive heat generation, showing a transition of the PTC effect to the NTC effect. Moreover, a micromechanical modeling was proposed to predict the occurrence of the PTC and NTC effects in the composites, considering various distances between CNTs and wavinesses of CNT. The change of the distance between CNTs under a heating condition was estimated, using the molecular dynamics software Material studio. Comparisons between the predictions and the experimental results were made to show the applicability of the proposed modeling scheme.

1. Introduction

Conductive polymeric composites (CPCs) have attracted significant attention as highly functional and advanced materials [1,2]. They have been used as supercapacitors, in health monitoring devices, and as electrostatic dissipation materials [3–5]. Applications of these composites can be diversified with various combinations of a polymer matrix and an electrically conductive filler material [1–5]. In particular, CPCs are capable of generating heat, through the principle of Joule heating, a process by which the passage of an electric current through a conductor produces heat [6,7]. Recently, CPCs have been investigated as self-heating elements in vehicles, textiles, and thermistors [8–10].

Carbon-based materials, such as carbon black, graphite, and carbon fiber, have been used extensively as electrically conductive fillers for the fabrication of CPCs [11–13]. Carbon nanotube (CNT) is very attractive for applications as an electrically conductive filler due to the inherent properties of this material. CNT has outstanding electrical and thermal conductivity values of 1.7 – 2.0E6 S/m and 3,000 W/mK, respectively [14–17]. In addition, the high aspect ratio of CNT can reduce the thermal contact resistance between the CNTs, generating a CNT microarchitecture [18]. This aspect ratio allows CPCs to exhibit excellent electrical conductivity and heating performance even at low CNT fractions in the CPCs [18,19].

Polypropylene is a widely used thermoplastic polymer matrix owing to its well-balanced mechanical properties, good chemical and corrosion resistance, and good processability at a relatively low cost [20,21]. Therefore, polypropylene has been actively utilized in the polymer matrix of CPCs for engineering applications. Recent studies of CNT-polypropylene composites have assessed the electrical properties of composites [22–24]. Logakis et al. [24] used CNT as an electrically conductive filler to fabricate conductive polypropylene composites, reporting that the composites showed lower electrical percolation threshold (0.6–0.7 vol.%) than previously reported results in similar systems.

Over the years, numerous studies have investigated the heat generation and heat-dependent electrical characteristics of CPCs under a self-heating condition [6,7,19,25,26]. CPCs used as self-heating elements undergo changes in their resistance levels with an increase in the temperature, typically referred to as positive temperature coefficient (PTC) or negative temperature coefficient (NTC) effects [6,26]. Several

* Corresponding author.
E-mail address: haengki@kaist.ac.kr (H.K. Lee).

https://doi.org/10.1016/j.compstruct.2022.115440
Received 20 July 2021; Received in revised form 22 February 2022; Accepted 2 March 2022
Available online 7 March 2022

researchers have demonstrated the influence of PTC and NTC effects on the reduced heating performance outcomes of CPCs under a self-heating condition [7,19]. In particular, the NTC effect can cause the electrically conductive fillers to overheat due to the reduction of electrical resistance, which leads to a thermal shock in the composites [7,27,28]. Despite several studies pertaining to the self-heating properties of CPCs, a comprehensive investigation of CNT-polypropylene composites to identify the self-heating characteristics of these composites has not been conducted.

The present study proposed a combined experimental and micromechanical approach to investigating PTC and NTC effects in CNT-polypropylene composites under a self-heating condition. The electrical and heating performance of film types of CNT-polypropylene composites was evaluated via electrical conductivity measurements and self-heating tests, while thermal transitions in the composites were observed by differential scanning calorimetry (DSC) tests. In addition, a micromechanical modeling was proposed to predict the occurrence of the PTC and NTC effects, which considers distances between CNTs and wavinesses of CNT with the increase of temperature. The change of the distance between CNTs under a heating condition was estimated, using the molecular dynamics (MD) software Material studio [29]. The present predictions were then compared with experimentally obtained values to verify the applicability of the proposed micromechanical modeling scheme.

2. Experimental procedure

2.1. Materials and test methods

Isotactic polypropylene (Sigma-Aldrich Inc.) was used as a base polymer matrix for the fabrication of the composites. Its average molecular weight and number were approximately 250,000 and 67,000, respectively. The melting point of polypropylene was in the temperature range of 160 to 165 °C. Multi-walled CNT (Hyosung Inc.) was used as an electrically conductive filler. The CNT was produced by the thermal chemical vapor deposition growth method [30], and the purity level of the CNT exceeded 95.0%. The length of the CNT was approximately 10.0 μm and the diameter ranges from 12.0 to 40.0 nm. Silica fume (Elkem Inc.) was used to detach the CNT aggregates mechanically [31]. The diameter of the silica fume particles ranged from 100 to 200 nm. A polycarboxylate-type superplasticizer (Dongnam Co., Ltd.) was also added to disperse the CNT in polypropylene [31]. Xylene solution (Samchun Inc.) was used as a solvent to dissolve the polypropylene particles uniformly.

The mix proportions of the composites are tabulated in Table 1. The composites were fabricated with various CNT contents. The amounts of the incorporated dispersion agents, i.e., silica fume and superplasticizer, were referenced from a previous study [31]. The fabrication of the composites consists of three steps. First, the CNT with dispersion agents was poured into 100 mL of xylene and sonicated for 1 h using tip-type ultra-sonication equipment (Sonic & Materials, USA), where the amplitude and the pulse on/off time were 17.5 μm and 10 s [32], respectively. The next step was to dissolve the polypropylene, which is the polymer matrix used in this study. To melt the polypropylene, 300 mL of xylene and 15 g of the polypropylene were stirred using a hotplate for 1 h at 260 °C until the polypropylene was totally dissolved [10]. The polypropylene solution and the CNT-dispersed solution obtained from the first step were then mixed at 200 °C for 3 h, until all of the xylene had evaporated entirely. Subsequently, the solid composites were dried at 70 °C for 24 h to solidify them completely. Finally, the fully dried solid composites were pressed to form a film-type condition. The solid composites were cut into particles with a radius of approximately 50.0 mm and put into a mold (100 mm × 100 mm × 0.5 mm) in a pressing machine with a thermostat. The temperature and pressure were increased to 220 °C and 40 MPa, respectively, and were maintained at these levels for 5 min. The film-type composites were then cooled to room temperature [10,26].

Table 1
Mix proportions of the composites (wt.%).

Specimen*	Polypropylene	CNT	Superplasticizer	Silica fume
Pure polypropylene	100	0	3.2	5.0
0.5-CNT	100	0.5	3.2	5.0
1.0-CNT	100	1.0	3.2	5.0
2.0-CNT	100	2.0	3.2	5.0
3.0-CNT	100	3.0	3.2	5.0
4.0-CNT	100	4.0	3.2	5.0
5.0-CNT	100	5.0	3.2	5.0

* Note that the digits included in the specimens' names denote their CNT contents (wt.%).

Fig. 1 shows an experimental procedure of the electrical conductivity measurement and the self-heating of the film-type CNT-polypropylene composites. The resistance of the composites was measured using the two-probe method with a digital multimeter (Keysight Technologies U1281A) [33]. Both sides of the fabricated film-type composites were covered with silver paste as electrodes and cut into ten replicas (10 mm × 10 mm × 0.5 mm) as shown in Fig. 1(a). The electrical resistance of the ten replicas was used to determine the average representative resistance value, which was then converted into the electrical conductivity using Eq. (1) [33,34]:

$$\sigma = \frac{L}{RA} \tag{1}$$

where σ is the electrical conductivity (S/m), R is the electrical resistance (Ω), A is the cross-sectional area (cm^2), and L is the distance between the sides of the composites (cm) [34].

A self-heating test was conducted to evaluate the heat generation and heat-dependent electrical characteristics in the composites. Pieces of the composites were cut into three replicas having dimensions of 5 mm × 30 mm × 0.5 mm. To ensure good electrical contact, silver paste was used to cover both ends of each specimen (5 mm × 5 mm). Copper tape was also attached onto the silver paste [26], and a direct current power supply was connected to the copper tape. To measure the surface temperature, a K-type thermocouple was attached onto the central surface of the composites and linked to a data logger (Agilent Technologies 34972A) as shown in Fig. 1(b). The electrical current value of the composites over time was recorded by manually applying a voltage from 9 to 18 V for 600 s [35]. After the test, the resistance (R) was calculated by dividing the electrical current by the input voltage. The normalized resistance (R/R_0) was obtained by dividing R by the initial resistance (R_0), which was measured immediately after the voltage was applied [7]. A DSC test (Mettler Toledo, DSC1) was conducted to measure the consolidation temperature of pure polypropylene and the composites. Samples (10 mg) were enclosed and heated from 20 to 200 °C at a heating rate of 10 °C/min in N_2 gas [24,35].

2.2. Results and discussion

The measured electrical conductivity of the composites with various CNT contents is shown in Fig. 2. The threshold in percolation theory is defined as the critical point at which the overall electrical conductivity of the composites shifts from the electrical conductivity of the matrix phase to that of the conductive filler phase as the conductive filler content increases further [26,36]. This phenomenon arises because the contact of adjacent conductive filler particles promotes the formation of continuous electrically conductive pathways [36]. This theory implies that the electrical conductivity of the composites increases noticeably near the percolation threshold as the amount of the conductive filler increases. In this experiment, the percolation threshold was observed in the specimens with a CNT content of less than 0.5 wt.% as the electrical conductivity increases sharply in the 0.5-CNT specimen. Beyond the

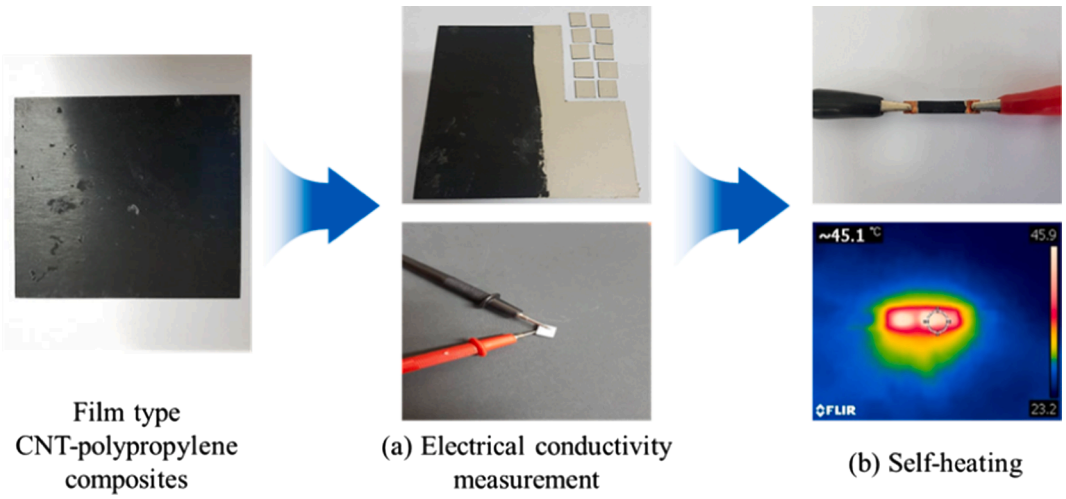

Fig. 1. Experimental procedure for (a) the electrical conductivity measurement and (b) the self-heating of the film type CNT-polypropylene composites.

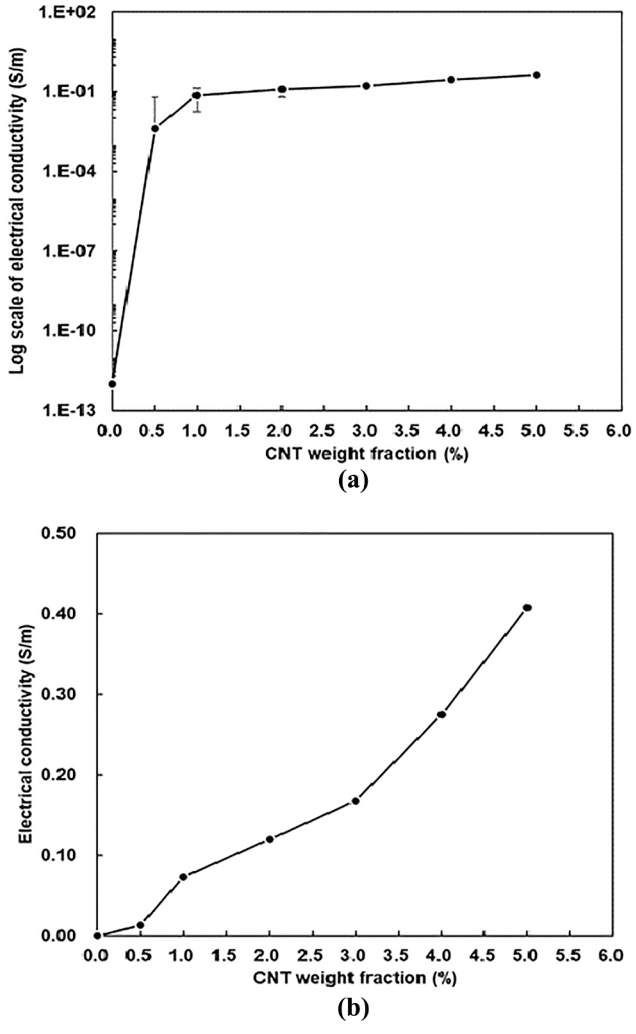

Fig. 2. Measured electrical conductivity of the composites with various CNT contents: (a) log scale and (b) normal scale.

percolation threshold, the electrical conductivity of the specimens increased constantly to 0.27 and 0.41 S/m for the 4.0-CNT and 5.0-CNT specimens, respectively.

The terminal surface temperatures of the composites at various input voltages after the self-heating test are shown in Fig. 3. Three replicas were used to determine the average terminal surface temperature (Fig. 3) in the self-heating test. The standard deviation value obtained from the three replicas was calculated to be less than 5.0%. The corresponding surface temperature and normalized resistance of the specimens are shown in Figs. 4 and 5, respectively. Although the electrical conductivity of the 1.0-CNT specimen was higher than that of the 0.5-CNT specimen as shown in Fig. 2, the difference of the surface temperature change between 0.5-CNT and 1.0-CNT specimens was not large (Fig. 3). It is likely that the electrically conductive pathways in composites having a dilute CNT content may not be sufficiently formed as reported elsewhere [7,19]. On the other hand, the terminal surface temperatures of the 2.0-CNT and 3.0-CNT specimens increased linearly with an increase in the input voltage, both ultimately reaching the terminal surface temperature of 60 °C at an input voltage level of 18 V. Meanwhile, the 4.0-CNT and 5.0-CNT specimens showed a drastic increase in the terminal surface temperature with an increase in the input voltage. It should be noted that one of the 5.0-CNT specimens was melted after the self-heating test, while two of the 5.0-CNT specimen were broken after the test, as shown in Fig. 3. Therefore, the self-heating test of the 5.0-CNT specimen could not be conducted at the input voltage of 18 V. These observations reveal that high input voltage was required for noticeable heat generation of the composites with CNT contents of

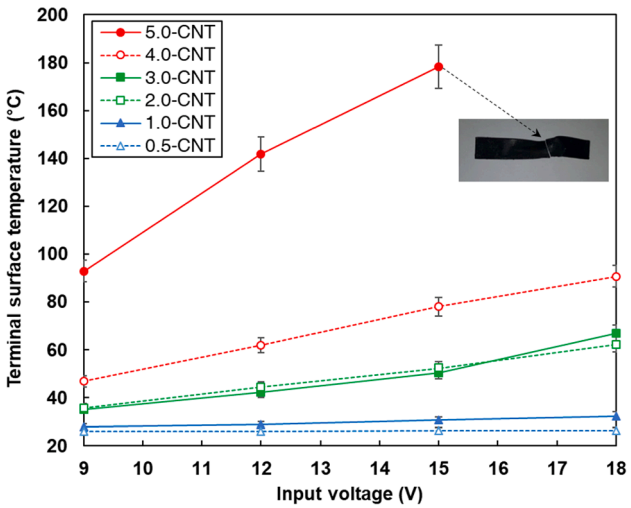

Fig. 3. Terminal surface temperatures of the composites at various input voltages after the self-heating test.

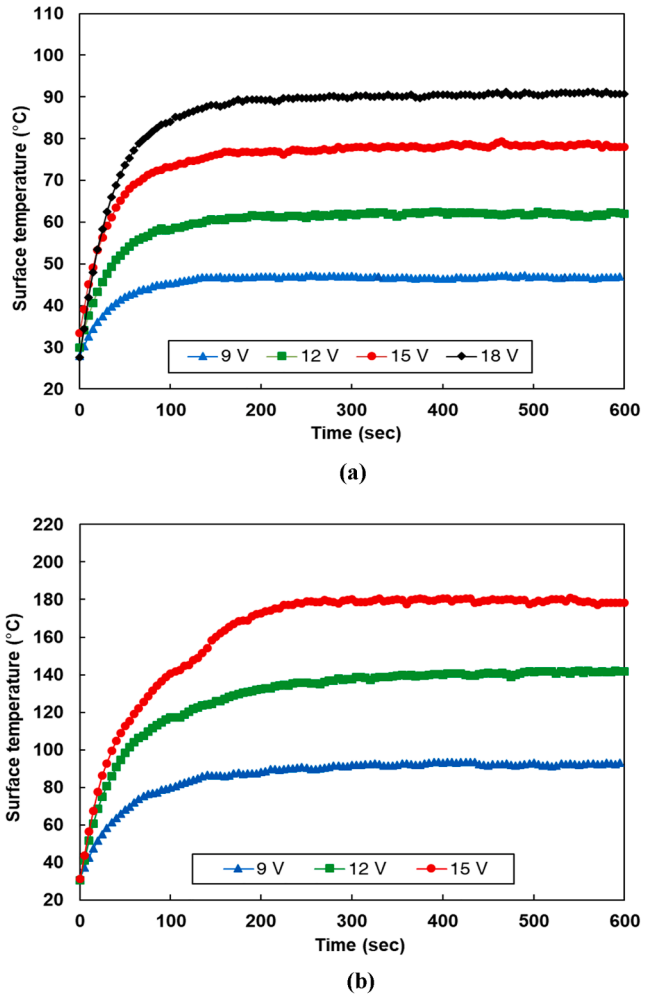

Fig. 4. Surface temperatures of (a) 4.0-CNT and (b) 5.0-CNT specimens over time.

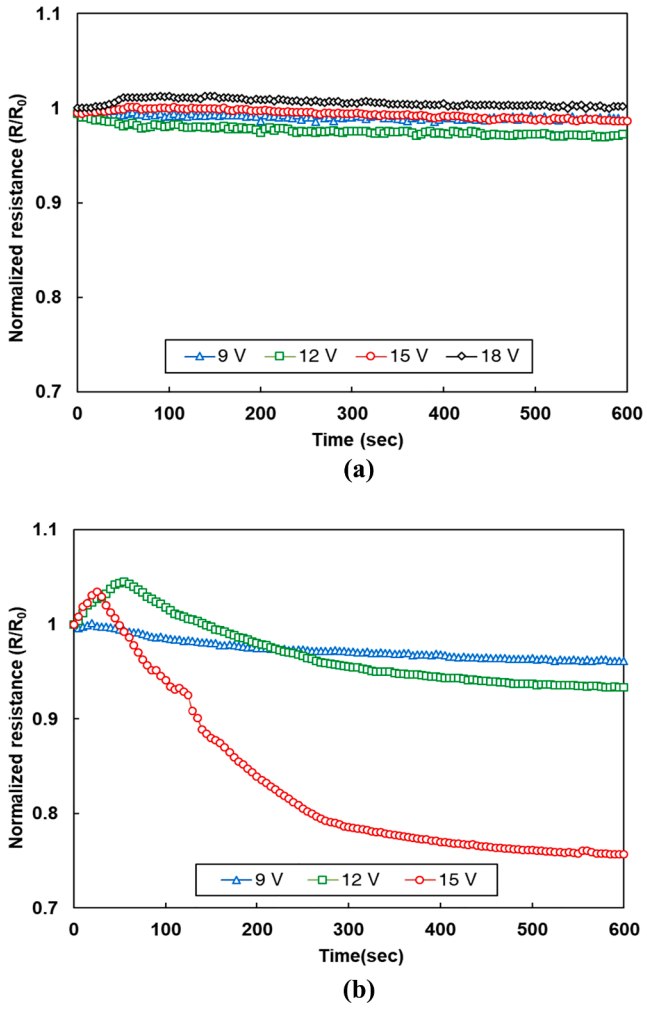

Fig. 5. Normalized resistances of (a) 4.0-CNT and (b) 5.0-CNT specimens over time.

less than 4.0 wt.% [6,7,19]. In relation to this, a self-heating test of the composites over time was carried out for the 4.0-CNT and 5.0-CNT specimens to investigate the PTC and NTC effects during the self-heating of these composites.

The surface temperatures of 4.0-CNT and 5.0-CNT specimens over time are shown in Fig. 4. The surface temperature of the 4.0-CNT specimen increased rapidly until 100 s at all voltages and soon become constant. The terminal surface temperatures were 46.9, 62.0, 78.1, and 90.7 °C at input voltages of 9, 12, 15, and 18 V, respectively. Meanwhile, the surface temperature of the 5.0-CNT specimen increased drastically until 200 s at all voltages. After 200 s, the surface temperature of the 5.0-CNT specimen slightly decreased at an input voltage of 15 V, while the surface temperature of the 5.0-CNT specimen became constant at input voltages of 9 and 12 V. The terminal surface temperatures were 92.4, 141.8, and 178.3 °C at input voltages of 9, 12, and 15 V, respectively. The terminal surface temperature of the 5.0-CNT specimen was approximately twice higher than those of the 4.0-CNT specimen at identical input voltages because the electrical conductivity of the 5.0-CNT specimen was higher than that of the 4.0-CNT specimen (see Fig. 2).

The normalized resistance values of 4.0-CNT and 5.0-CNT specimens over time are shown in Fig. 5. The change in the normalized resistance of the 4.0-CNT specimen at input voltages of 9, 12, and 15 V was negligible. However, the normalized resistance value of the 5.0-CNT specimen at the input voltages of 12 and 15 V increased momentarily until 50 s and 20 s, respectively, with an increase in the temperature, which can be interpreted as the PTC effect, i.e., an increase in the electrical resistivity of CPCs with an increase in the temperature [26]. In general, the PTC effect has been reported to appear in composites consisting of a polymer and electrically conductive fillers, such as carbon black and carbon fiber [6,10]. Nakano et al. [26] found that the PTC effect occurs due to a relative decrease in the filler content in relation to the volume caused by the thermal expansion of the base polymer, which disconnects the electrically conductive pathways within the composites. Accordingly, the abrupt increase in the temperature of the 5.0-CNT specimen is very likely to cause a thermal expansion of the polypropylene, which could lead to the disconnection of the electrically conductive pathways in the polypropylene and to an increase in the normalized resistance, thus initiating the PTC effect [26]. Meanwhile, after a small increase in the normalized resistance at the input voltages of 12 and 15 V, the normalized resistance of the 5.0-CNT specimen decreased drastically until the end of the test period as shown in Fig. 5(b). These phenomena are closely associated with the NTC effect [7,19,28]. Isaji et al. [35] reported that the NTC effect is likely due to the considerable mobility of the polymer chains, which causes the CNT to stretch and close. This implies that the rearrangement of the CNT at a high temperature leads to the NTC effect, generating more electrical contact points.

The thermal transitions in the composites were analyzed by the DSC tests. Fig. 6(a) shows the crystallization thermograms of pure polypropylene, 4.0-CNT, and 5.0-CNT specimens at a cooling rate of 10 °C/min. The crystalline temperature of the pure polypropylene specimen appeared at 113.7 °C, while that of the 4.0-CNT and 5.0-CNT specimens

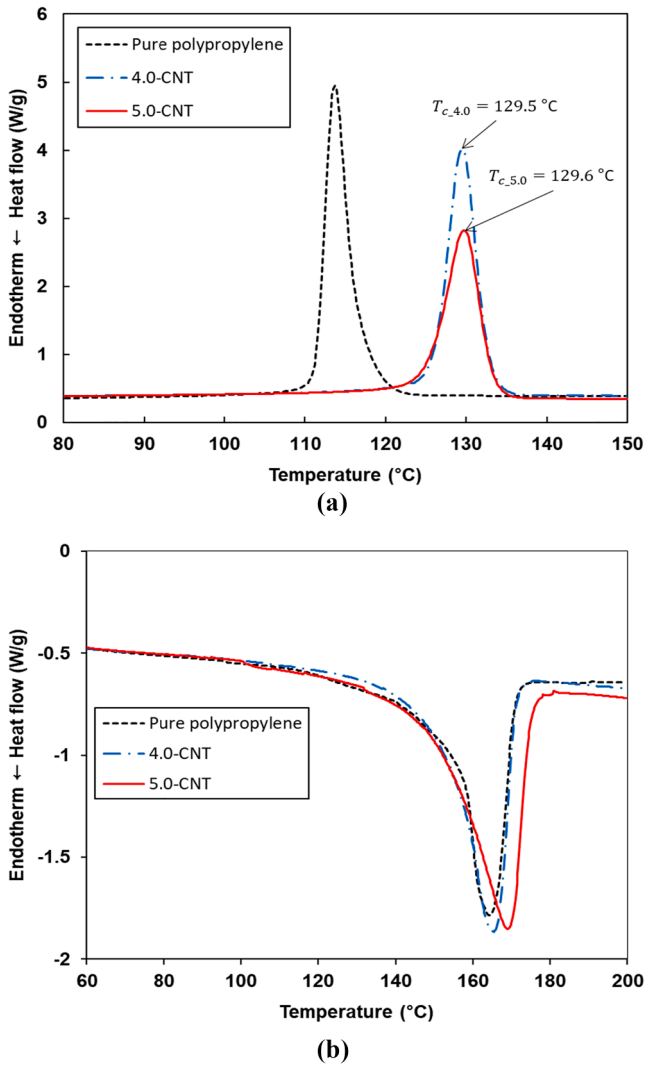

Fig. 6. (a) Crystallization thermograms (cooling rate: 10 °C/min) and (b) melting thermograms (heating rate: 10 °C /min) for pure polypropylene, 4.0-CNT, and 5.0-CNT specimens.

appeared at 129.5 and 129.6 °C, respectively. These results correspond well with the study made by Seo et al. [37], who reported that the addition of CNT enhances the nucleation process on polypropylene crystallization. This implies that the mobility of the polypropylene chains in the composites can considerably increase beyond the crystalline temperature (around 130 °C) since the crystalline polypropylene in the composites is changed to an amorphous state. Therefore, the measured crystalline temperature values of the specimens as denoted by "$T_{c\_4.0}$" and "$T_{c\_5.0}$" in Fig. 6(a) are considered as the temperature at which the NTC effect occurs in our theoretical modeling. In Fig. 6(b), melting thermograms of the pure polypropylene, the 4.0-CNT, and 5.0-CNT specimens at a heating rate of 10 °C/min are presented. The melting points of the pure polypropylene, the 4.0-CNT, and 5.0-CNT specimens were 164.3, 165.3, and 169.0 °C, respectively. These results are similar to the previous studies in that no significant changes in the melting point of the pure polypropylene phase were observed in the CNT-incorporated composites [24,37]. In addition, it can be said from these results that the 5.0-CNT specimens were melted or broken at input voltages of higher than 15 V since the surface temperature exceeded the melting point of the specimens.

3. Theoretical modeling

3.1. Micromechanical modeling

The micromechanical modeling was conducted to predict the occurrence of the PTC and NTC effects in the 5.0-CNT specimen because the change of the normalized resistance in the only 5.0-CNT specimen was noticeable in the experimental results. The electrical conductivity of CNT-polypropylene composites was estimated by adopting the effective medium theory based on micromechanics [38,39]. Wang et al. [38] developed a micromechanical model for predicting the electrical conductivity of the CNT-composites. The equations with more details on the electrical conductivity of CNT-composites can be seen by Wang et al. [38]. The CNT was assumed to be thinly coated to consider interfacial resistivity ρ. The effective electrical conductivity of the CNT considering the interfacial resistivity due to the tunneling effect $\widehat{\sigma_i}^C$ can be expressed by Eqs. (2) and (3) as reported in [38–40]:

$$\widehat{\sigma_i}^C = \frac{{\sigma_i}^C}{1 + \rho {\sigma_i}^C S_{ii}(D_e/L_e + 2)/(D_e/2)} \tag{2}$$

with

$$\rho = \frac{h^2 d_{CNT}}{e^2\sqrt{2m\lambda}} exp\left(\frac{4\pi d_{CNT}}{h}\sqrt{2m\lambda}\right) \tag{3}$$

where ${\sigma_i}^C$ (i = 1 and 3) correspondingly represent the electrical conductivity values of the CNT along the in-plane and normal directions not considering the interfacial resistivity [38,39]; S_{11}, S_{22}, and S_{33} are the components of the Eshelby's tensor for a spheroidal inclusion [38,39]; L_e and D_e represent the effective length and diameter of the CNT, respectively; d_{CNT} denote the distance between the CNTs in the matrix [40]; and e, m, h, and λ are the quantum of electricity, the mass of an electron, the Plank's constant, the height of the barrier, respectively [40].

Based on the experimental results, several assumptions were considered to predict the occurrence of the PTC and NTC effects in the composites. The assumptions were as follows: (1) the occurrence of the PTC and NTC effects is related to the increase in the temperature of the composites over time $T(t)$; (2) d_{CNT} increases as the composites expand with an increase in the temperature until $T(t)$ reaches the crystalline temperature of the composites T_c from initial temperature (25 °C); (3) L_e starts to increase as $T(t)$ exceeds T_c since the waviness of the CNT reduces due to the increased mobility of the polypropylene chains in the composites. The aforementioned assumptions can be applied by defining d_{CNT}, L_e, and D_e with Eqs. (4)-(6) below as describes in [41–43]:

$$d_{CNT} = \left\{ d_i \bullet \alpha(T(t))(T(t) < T_c) d_i \bullet \alpha(\mathrm{T_c})(\mathrm{T(t)} \geq \mathrm{T_c}) \right. \tag{4}$$

$$L_e = \left\{ \frac{2\pi}{\tan\theta \bullet L(\theta_i)}\ (T(t) < T_c) \frac{2\pi}{\tan\theta \bullet L(\theta_i)} \bullet (1 + \gamma \bullet (\mathrm{t - t_c}))(\mathrm{T(t)} \geq \mathrm{T_c}) \right. \tag{5}$$

$$D_e = \frac{D}{2} + \frac{L}{L(\theta_i)} \tag{6}$$

where d_i and θ_i denote the initial distance between the CNTs and the initial waviness of the CNT, respectively; L and D are the length and diameter of the CNT, respectively; $\alpha(T(t))$ correspondingly represents the ratio of the distance change between the CNTs in composites at $T(t)$, which will be described in Section 3.2; t_c signifies the specific time at which $T(t)$ reaches T_c; and γ represents the scale parameter which is related to the stretching ratio of the CNT [42,43]. The initial length of the CNT considering CNT waviness $L(\theta_i)$ can be found in [41]. Note that the d_i, θ_i, and γ are parameters in the present model.

The temperature of the composites over time $T(t)$ can be estimated

with Eq. (7) as in [6]:

$$T(t) = (T_{max} - T_0) \bullet \left(1 - e^{-\frac{t}{\tau_g}}\right) \quad (7)$$

where T_{max} and T_0 denote the maximum and the initial temperatures, respectively. τ_g indicates the characteristic growth time constant [6]. Here, the experimental results in Section 2 were inputted to T_{max} and T_0 values, respectively. τ_g values were determined by fitting to the present experimental results [6]. The fitted τ_g values were 27, 25, and 23 at input voltages of 9, 12, and 15 V, respectively.

3.2. Molecular dynamics simulation

The MD simulation was conducted to investigate the thermal behavior of the composites under a heating condition. The MD simulation is a powerful computational experiment tool to understand the behavior of polymeric composites at an atomic scale [44]. It can demonstrate the full atomistic mechanism at the heterogeneous interface between CNT and polymer matrix with little empiricism [45]. Therefore, in this study, d_{CNT} under a heating condition was estimated using the MD software Material studio [29].

A molecular unit cell with a 5.0 vol.% of CNT was constructed in this study in accordance with the earlier work [45–47], which modeled the representative volume element of the CNT-polypropylene composites. The model parameters and conditions utilized in the present MD simulation [44–47] are listed in Table 2. Fig. 7 shows molecular structures of (a) a polypropylene chain, (b) a CNT, and (c) the 5.0-CNT specimen. In this study, amorphous isotactic polypropylene has been modeled by assembling twenty-unit monomers [45]. A zigzag type CNT with a chiral vector of (5,0) was considered, and their diameter and length were 3.9 and 42.6 Å, respectively [45,46]. The molecular unit cell of the 5.0-CNT specimen was composed of a centered CNT and 54 polypropylene chains with a target density of 0.8 g/cm^3, which are close to the experimental density of the 5.0-CNT specimen. The side length of the cubic unit cell is 46.3 Å, and periodic boundary conditions were imposed in all directions. Then, the total potential energy of the unit cell was minimized via the conjugate gradient method with the specific maximum energy change of 0.001 kcal/mol [46]. All the cell construction and the subsequent energy minimization process were performed using a COMPASS forcefield.

After sufficiently minimizing initial structures, the unit cell was equilibrated at 1 atm and 200 K via the grand canonical, *NPT*, ensemble simulation where the *N, P*, and *T* indicate the number of atoms, the pressure, and temperature, respectively [45]. After the equilibrium was finished, three cycles of *NPT* simulation were conducted heating 300 to 450 K by a step of 25 K where the pressure of the system was conserved to 1 atm to obtain the change of the cell volume with the increase of temperature [48]. At each increase in temperature, the average cell volume *V* was calculated. The specific cell volume (V/V_0) was obtained by dividing *V* by the cell volume V_0 at 25 °C. The specific cell volume of the 5.0-CNT specimen with temperature (the average values obtained by

Table 2
Model parameters and conditions utilized in the present MD simulation [45–47].

Parameter and condition	Present simulation
Number of polypropylene chains	54
CNT volume fraction (vol.%)	5.0
CNT diameter (Å)	3.9
CNT length (Å)	42.6
Target density (g/cm^3)	0.8
Cell size (Å^3)	46.3 × 46.3 × 46.3
Total number of atoms	10,028
Forcefield	COMPASS
MD ensemble	NPT
Pressure (atm)	1
Pressure control method	Berendsen

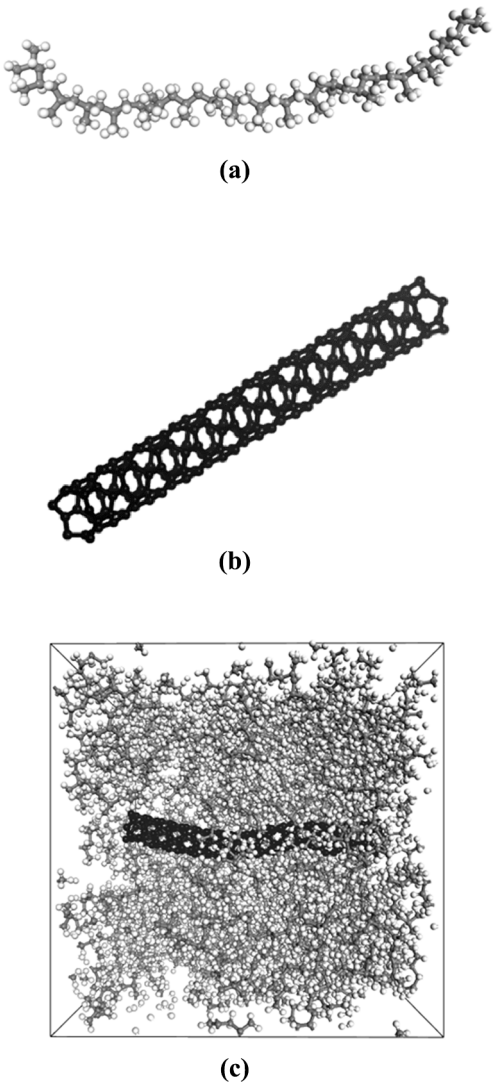

Fig. 7. Molecular structures of (a) a polypropylene chain, (b) a CNT, and (c) the 5.0-CNT specimen.

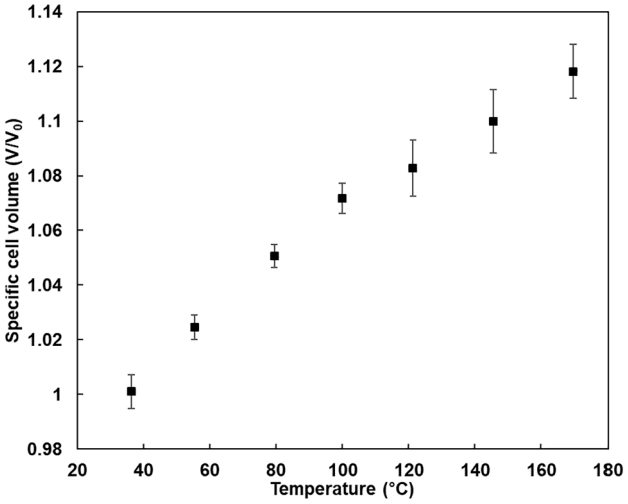

Fig. 8. Specific cell volume of the 5.0-CNT specimen with temperature (the average value obtained by the MD simulation).

the MD simulation) is shown in Fig. 8. Here, we assumed that the specific cell length at $T(t)$ is identical to the ratio of the distance change between the CNTs in composites at $T(t)$. Accordingly, the specific cell length estimated through linear regression in Fig. 8 was inputted to $\alpha(T(t))$ in Eq.(4).

However, it should be noted that a single-walled carbon nanotube with anisotropic polypropylene chains was modeled in this study with a periodic boundary condition due to the computational limitations in considering a huge number of atoms in the unit cell simulation which is identical to the 5.0-CNT specimen. In order to improve the computational accuracy of the MD simulation, averaging schemes and repetitive calculations were conducted [45]. In addition, since the shape of the CNT incorporated in the matrix was assumed to be straight in the present MD simulation, the MD simulation could not consider the effects of the waviness and aggregation of the CNT under a heating condition.

3.3. Parametric studies and experimental comparison

The normalized resistance of the composites with various initial distances between the CNTs, initial wavinesses of the CNT, and scale parameters was simulated. Note that these parametric studies were conducted to predict the occurrence of the PTC and NTC effects of the 5.0-CNT specimen at the input voltage of 15 V. The material and model parameters were: $L = 10.0$ μm, $D = 26.0$ nm, $\sigma_0 = 1.0\text{E-}12$ S/m, ${\sigma_1}^C = 1.9\text{E}4$ S/m, $\lambda = 0.5$ eV, and $\alpha(T(t)) = 0.003T + 0.9$ [22,27,40]. The value of ${\sigma_3}^C$ was assumed to be expressed by ${\sigma_3}^C = 1000{\sigma_1}^C$ [27]. e, m, and h were referenced from a previous study [40].

The normalized resistance of the 5.0-CNT specimen with various d_i is simulated, as shown in Fig. 9(a). According to the literature [49], a parametric study of d_i with normalized resistance was conducted by selecting a range of values from 0.4 to 0.6 nm. The PTC and NTC effects appeared noticeably and the height of the peak increased as d_i increases. In particular, d_i= 0.4 nm showed a slight increase of the normalized resistance because the distance of CNTs is highly close, which could not influence the change of electrical resistance. The results in Fig. 9(a) show that d_i plays an important role in predicting the occurrence of the PTC effect.

The normalized resistance of the 5.0-CNT specimen for various θ_i and γ is shown in Fig. 9(b) and (c). Earlier work in the literature selected a range of θ_i between 4.0 and 10.0° [41,50,51]. Hence, a parametric study of θ_i with normalized resistance was conducted by selecting a range of values from 5.0 to 7.0°. A larger value of θ_i led to lower normalized resistance at 600 s, while the magnitude of the peak did not change as θ_i increases. These results indicate that using CNT with a higher θ_i led to a drastic NTC effect due to the decrease of the effective aspect ratio of the CNT in Eq. (5) [42]. Fig. 9(c) shows the normalized resistance of the 5.0-CNT specimen with various γ at an input voltage of 15 V. The NTC effect appeared remarkably as γ increases. In particular, the case of $\gamma =$ 5.0E-3 showed that the normalized resistance decreases significantly after the peak. A higher value of γ resulted in a more rapid NTC effect, increasing the stretching ratio of the CNT in Eq. (5). Therefore, the results in Fig. 9 (b) and (c) show that both model parameters θ_i and γ were important factors affecting the slope of the NTC effect [42].

The comparisons of the normalized resistance of the 5.0-CNT specimen between the predictions and the experimental results are shown in Fig. 10. Based on the parametric studies, model parameters for an input voltage of 15 V were assumed as follows: $d_i = 0.55$ nm, $\theta_i =$ 7.0°, and $\gamma =$ 3.0E-3, while γ values for an input voltage of 9 and 12 V were estimated to be 4.0E-4 and 5.0E-5, respectively. Both predictions for input voltages of 12 and 15 V showed that the peak representing the PTC effect and the change of normalized resistance over time were in good agreement with the experimental results. However, the difference between the predictions and the experimental results was higher in the specimen at an input voltage of 9 V compared to those in the specimens at other input voltages. This observation may be associated with the

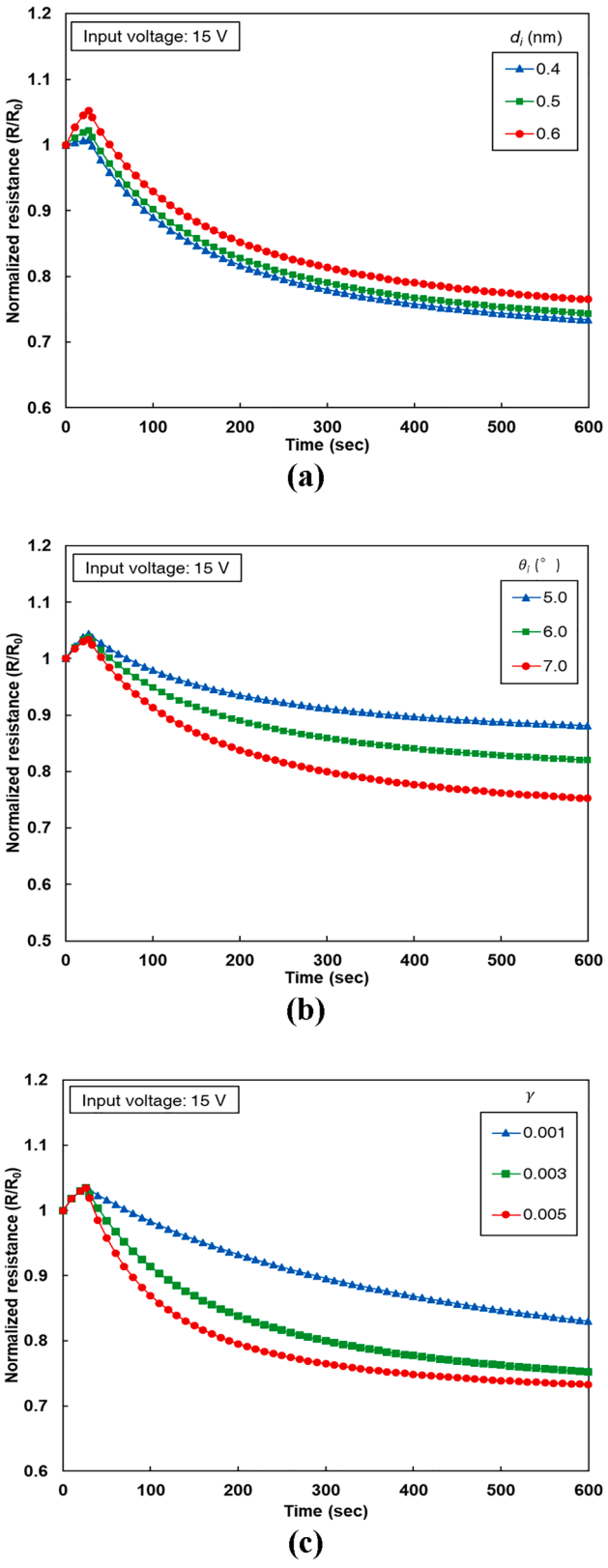

Fig. 9. Normalized resistance of the 5.0-CNT specimen with various (a) initial distances between the CNTs, (b) initial wavinesses of the CNT, and (c) scale parameters at an input voltage of 15 V.

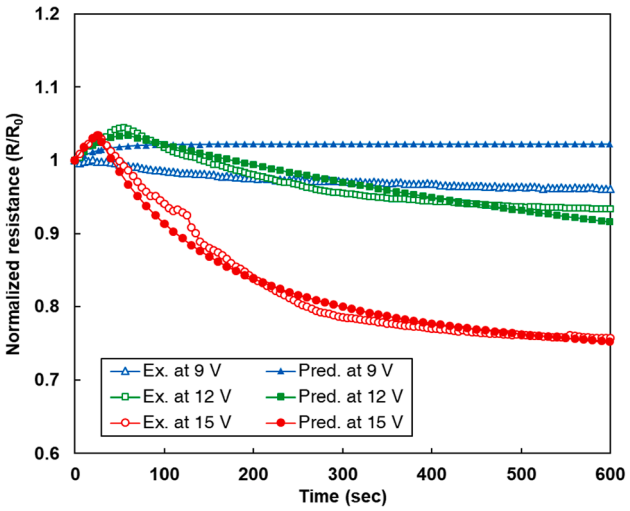

Fig. 10. Comparisons of the normalized resistance of the 5.0-CNT specimen between the predictions and the experimental results.

assumption that d_{CNT} increases linearly in the composites before $T(t)$ reaches the crystalline temperature. Through the comparisons between the present predictions and the experimental results, the proposed modeling was shown to be able to predict the occurrence of the PTC and NTC effects in CNT-polypropylene composites under the self-heating condition.

4. Concluding remarks

A combined experimental and micromechanical approach to investigating PTC and NTC effects in CNT-polypropylene composites under a self-heating condition was proposed in this study. The electrical and heating performance of the composites were evaluated by electrical conductivity measurements as well as self-heating tests. The PTC and NTC effects in the composites were discussed in parallel with changes in the normalized resistance. In addition, a micromechanical modeling integrated MD simulation was carried out to predict the occurrence of the PTC and NTC effects in the composites. The key findings of the study can be summarized below.

(1) Although the terminal surface temperatures of the 5.0-CNT specimens after the self-heating test at 12 and 15 V were increased to 141.8 and 178 °C, respectively, the 5.0-CNT specimens showed a transition of the PTC effect to the NTC effect at input voltages of higher than 12 V.
(2) The normalized resistance of composites having higher CNT contents (e.g. 5.0 wt.%) during the self-heating test at 15 V was severely decreased with an increase in the surface temperature, showing the occurrence of the rapid NTC effect. It can be said from the DSC results that the CNT rearrangement caused by the considerable mobility of the polypropylene chains at a high temperature can lead to the NTC effect, generating more electrical contact points in the composites.
(3) The parametric studies of the micromechanical modeling integrated MD simulation demonstrated that the initial distance between the CNTs, the initial waviness of the CNT, and the scale parameter all played important roles in predicting the PTC and NTC effects. The predicted normalized resistance outcomes using the model parameters obtained from the parametric studies were in good agreement with experimental results.

It is expected that the combined experimental and micromechanical approach can be used to investigate the PTC and NTC effects in CNT-polypropylene composites under the self-heating condition. However, the range of parameters in the present model was assumed by referring to the outcomes reported in the previous works, and thus relevant experimental schemes capable of determining the value of parameters in the present model may be needed for more accurate and realistic predictions.

CRediT authorship contribution statement

Taegeon Kil: Conceptualization, Investigation, Data curation, Resources, Writing – original draft. **D.W. Jin:** Methodology, Visualization, Formal analysis. **Beomjoo Yang:** Software, Validation, Writing – review & editing. **H.K. Lee:** Supervision, Project administration, Funding acquisition.

Declaration of Competing Interest

The authors declare that they have no known competing financial interests or personal relationships that could have appeared to influence the work reported in this paper.

Acknowledgments

This research was supported by a grant from the National Research Foundation of Korea (NRF) funded by the Korean government (Ministry of Science, ICT & Future Planning) (NRF- 2021R1A2C3006382) and by the Hyundai Motor Group (Future Technology Research Project). The authors thank Mr. J.H. Seo at KAIST for proofreading.

References

[1] Park HK, Kim SM, Lee JS, Park JH, Hong YK, Hong CH, et al. Flexible plane heater: Graphite and carbon nanotube hybrid nanocomposite. Synth Met 2015;203:127–34.
[2] Bauhofer W, Kovacs JZ. A review and analysis of electrical percolation in carbon nanotube polymer composites. Compos Sci Technol 2009;69(10):1486–98.
[3] Lin L, Liu S, Zhang Q, Li X, Ji M, Deng H, et al. Towards tunable sensitivity of electrical property to strain for conductive polymer composites based on thermoplastic elastomer. ACS Appl Mater Interfaces 2013;5(12):5815–24.
[4] Böger L, Wichmann MH, Meyer LO, Schulte K. Load and health monitoring in glass fibre reinforced composites with an electrically conductive nanocomposite epoxy matrix. Compos Sci Technol 2008;68(7–8):1886–94.
[5] Jang D, Yoon HN, Seo J, Park S, Kil T, Lee HK. Improved electric heating characteristics of CNT-embedded polymeric composites with an addition of silica aerogel. Compos Sci Technol 2021;212:108866.
[6] Yan J, Jeong YG. Multiwalled carbon nanotube/polydimethylsiloxane composite films as high performance flexible electric heating elements. Appl Phys Lett 2014;105(5):051907.
[7] Kil T, Jang DI, Yoon HN, Yang B. Machine Learning-Based Predictions on the Self-Heating Characteristics of Nanocomposites with Hybrid Fillers. Comput Mater Contin 2022;71(3):4487–502.
[8] Yoon YH, Song JW, Kim D, Kim J, Park JK, Oh SK, et al. Transparent film heater using single-walled carbon nanotubes. Adv Mater 2007;19(23):4284–7.
[9] Varesano A, Tonin C. Improving electrical performances of wool textiles: synthesis of conducting polypyrrole on the fiber surface. Text Res J 2008;78(12):110–1115.
[10] Zeng Y, Lu G, Wang H, Du J, Ying Z, Liu C. Positive temperature coefficient thermistors based on carbon nanotube/polymer composites. Sci Rep 2014;4:6684.
[11] Zhang D, Ye L, Deng S, Zhang J, Tang Y, Chen Y. CF/EP composite laminates with carbon black and copper chloride for improved electrical conductivity and interlaminar fracture toughness. Compos Sci Technol 2012;72(3):412–20.
[12] Song LN, Xiao M, Meng YZ. Electrically conductive nanocomposites of aromatic polydisulfide/expanded graphite. Compos Sci Technol 2006;66(13):2156–62.
[13] Kumar S, Rath T, Mahaling RN, Reddy CS, Das CK, Pandey KN, et al. Study on mechanical, morphological and electrical properties of carbon nanofiber/polyetherimide composites. Mater Sci Eng B 2007;141(1-2):61–70.
[14] Ebbesen TW, Lezec HJ, Hiura H, Bennett JW, Ghaemi HF, Thio T. Electrical conductivity of individual carbon nanotubes. Nature 1996;382(6586):54–6.
[15] Kim P, Shi L, Majumdar A, McEuen PL. Thermal transport measurements of individual multiwalled nanotubes. Phys Rev Lett 2001;87(21):215502.
[16] Lee SH, Lee DH, Lee WJ, Kim SO. Tailored assembly of carbon nanotubes and graphene. Adv Funct Mater 2011;21(8):1338–54.
[17] Berber S, Kwon Y-K, Tománek D. Unusually high thermal conductivity of carbon nanotubes. Phys Rev Lett 2000;84(20):4613–6.
[18] Bozlar M, He D, Bai J, Chalopin Y, Mingo N, Volz S. Carbon nanotube microarchitectures for enhanced thermal conduction at ultralow mass fraction in polymer composites. Adv Mater 2010;22(14):1654–8.
[19] Chu K, Park SH. Electrical heating behavior of flexible carbon nanotube composites with different aspect ratios. J Ind Eng Chem 2016;35:195–8.

[20] Pan Y, Li L, Chan SH, Zhao J. Correlation between dispersion state and electrical conductivity of MWCNTs/PP composites prepared by melt blending. Compos Part A Appl Sci Manuf 2010;41(3):419–26.
[21] Ma Y, Wu D, Liu Y, Li X, Qiao H, Yu ZZ. Electrically conductive and super-tough polypropylene/carbon nanotube nanocomposites prepared by melt compounding. Compos Part B-Eng 2014;56:384–91.
[22] Kil T, Jin DW, Yang B, Lee HK. A comprehensive micromechanical and experimental study of the electrical conductivity of polymeric composites incorporating carbon nanotube and carbon fiber. Compos Struct 2021;268:114002.
[23] Zhao J, Dai K, Liu C, Zheng G, Wang B, Liu C, et al. A comparison between strain sensing behaviors of carbon black/polypropylene and carbon nanotubes/polypropylene electrically conductive composites. Compos Part A Appl Sci Manuf 2013;48:129–36.
[24] Logakis E, Pollatos E, Pandis Ch, Peoglos V, Zuburtikudis I, Delides CG, et al. Structure–property relationships in isotactic polypropylene/multi-walled carbon nanotubes nanocomposites. Compos Sci Technol 2010;70(2):328–35.
[25] Naeemi A, Meindl JD. Physical modeling of temperature coefficient of resistance for single-and multi-wall carbon nanotube interconnects. IEEE Electron Device Lett 2007;28(2):135–8.
[26] Nakano H, Shimizu K, Takahashi S, Kono A, Ougizawa T, Horibe H. Resistivity–temperature characteristics of filler-dispersed polymer composites. Polym 2012;53(26):6112–7.
[27] Kim GM, Yang BJ, Yoon HN, Lee HK. Synergistic effects of carbon nanotube and carbon fiber on heat generation and electrical characteristics of cementitious composites. Carbon N Y 2018;134:283–92.
[28] Xiang ZD, Chen T, Li ZM, Bian XC. Negative temperature coefficient of resistivity in lightweight conductive carbon nanotube/polymer composites. Macromol Mater Eng 2009;294(2):91–5.
[29] Accelrys Inc, San Francisco.
[30] Biro LP, Khanh NQ, Vertesy Z, Horvath ZE, Osvath Z, Koos A, et al. Catalyst traces and other impurities in chemically purified carbon nanotubes grown by CVD. Mater Sci Eng C 2002;19(1–2):9–13.
[31] Kim GM, Kil T, Lee HK. A novel physicomechanical approach to dispersion of carbon nanotubes in polypropylene composites. Compos Struct 2021;258:113377.
[32] Krause B, Mende M, Pötschke P, Petzold G. Dispersability and particle size distribution of CNTs in an aqueous surfactant dispersion as a function of ultrasonic treatment time. Carbon 2010;48(10):2746–54.
[33] Cao J, Chung DDL. Electric polarization and depolarization in cement-based materials, studied by apparent electrical resistance measurement. Cement Concrete Res 2004;34(3):481–5.
[34] Liu H, Gao J, Huang W, Dai K, Zheng G, Liu C, et al. Electrically conductive strain sensing polyurethane nanocomposites with synergistic carbon nanotubes and graphene bifillers. Nanoscale 2016;8(26):12977–89.
[35] Isaji S, Bin Y, Matsuo M. Electrical conductivity and self-temperature-control heating properties of carbon nanotubes filled polyethylene films. Polym 2009;50(4):1046–53.
[36] Kim HK, Nam IW, Lee HK. Enhanced effect of carbon nanotube on mechanical and electrical properties of cement composites by incorporation of silica fume. Comp Struct 2014;107:60–9.
[37] Seo MK, Lee JR, Park SJ. Crystallization kinetics and interfacial behaviors of polypropylene composites reinforced with multi-walled carbon nanotubes. Mater Sci Eng A 2005;404(1–2):79–84.
[38] Wang Y, Weng GJ, Meguid SA, Hamouda AM. A continuum model with a percolation threshold and tunneling-assisted interfacial conductivity for carbon nanotube-based nanocomposites. J Appl Phys 2014;115(19):193706.
[39] Wang Y, Weng GJ. Electrical conductivity of carbon nanotube-and graphene-based nanocomposites. In: Meguid SA, Weng GJ, editors. Micromechanics and Nanomechanics of Composite Solids. Cham: Springer International Publishing; 2018. p. 123–56.
[40] Hu N, Karube Y, Yan C, Masuda Z, Fukunaga H. Tunneling effect in a polymer/carbon nanotube nanocomposite strain sensor. Acta Mater 2008;56(13):2929–36.
[41] Kim GM, Yang BJ, Cho KJ, Kim EM, Lee HK. Influences of CNT dispersion and pore characteristics on the electrical performance of cementitious composites. Compos Struct 2017;164:32–42.
[42] Wang X, Bradford PD, Liu W, Zhao H, Inoue Y, Maria J-P, et al. Mechanical and electrical property improvement in CNT/Nylon composites through drawing and stretching. Compos Sci Technol 2011;71(14):1677–83.
[43] Knox JH, McCormack KA. Volume expansion and loss of sample due to initial self-heating in capillary electroseparation (CES) systems. Chromatographia 1994;38(5-6):279–82.
[44] Yang BJ, Shin H, Lee HK, Kim H. A combined molecular dynamics/micromechanics/finite element approach for multiscale constitutive modeling of nanocomposites with interface effects. Appl Phys 2013;103(24):241903.
[45] Yang S, Yu S, Ryu J, Cho JM, Kyoung W, Han DS, et al. Nonlinear multiscale modeling approach to characterize elastoplastic behavior of CNT/polymer nanocomposites considering the interphase and interfacial imperfection. Int J Plast 2013;41:124–46.
[46] Yang S, Yu S, Kyoung W, Han DS, Cho M. Multiscale modeling of size-dependent elastic properties of carbon nanotube/polymer nanocomposites with interfacial imperfections. Polym 2012;53(2):623–33.
[47] Alian AR, Kundalwal SI, Meguid SA. Interfacial and mechanical properties of epoxy nanocomposites using different multiscale modeling schemes. Compos Struct 2015;131:545–55.
[48] Meunier M. Diffusion coefficients of small gas molecules in amorphous cis-1, 4-polybutadiene estimated by molecular dynamics simulations. J Chem Phys 2005;123(13):134906.
[49] Zare Y, Rhee KY. Simulation of percolation threshold, tunneling distance, and conductivity for carbon nanotube (CNT)-reinforced nanocomposites assuming effective CNT concentration. Polym 2020;12(1):114.
[50] Yazdchi K, Salehi M. The effects of CNT waviness on interfacial stress transfer characteristics of CNT/polymer composites. Compos Part A Appl Sci Manuf 2011;42(10):1301–9.
[51] Fisher FT, Bradshaw RD, Brinson LC. Fiber waviness in nanotube-reinforced polymer composites—I: Modulus predictions using effective nanotube properties. Compos Sci Technol 2003;63(11):1689–703.